Hindawi Publishing Corporation
International Journal of Mathematics and Mathematical Sciences
Volume 2008, Article ID 350326, 20 pages
doi:10.1155/2008/350326

Research Article

The Schwarz-Christoffel Conformal Mapping for "Polygons" with Infinitely Many Sides

Gonzalo Riera, Hernán Carrasco, and Rubén Preiss

Departamento de Matemáticas, Pontificia Universidad Católica de Chile, Avenue Vicuña Makenna 4860, 7820436 Macul, Santiago, Chile

Correspondence should be addressed to Gonzalo Riera, griera@mat.puc.cl

Received 22 January 2008; Revised 15 May 2008; Accepted 1 July 2008

Recommended by Vladimir Mityushev

The classical Schwarz-Christoffel formula gives conformal mappings of the upper half-plane onto domains whose boundaries consist of a finite number of line segments. In this paper, we explore extensions to boundary curves which in one sense or another are made up of infinitely many line segments, with specific attention to the "infinite staircase" and to the Koch snowflake, for both of which we develop explicit formulas for the mapping function and explain how one can use standard mathematical software to generate corresponding graphics. We also discuss a number of open questions suggested by these considerations, some of which are related to differentials on hyperelliptic surfaces of infinite genus.

1. Introduction

Let D be a polygon in the complex plane with n vertices and interior angles $\pi\alpha_i$, $0 \leq \alpha_i \leq 2$, $1 \leq i \leq n$; the exterior angles are given by $\pi\mu_i$, where $\alpha_i + \mu_i = 1$. The Schwarz-Christoffel mapping of the upper-half plane onto D is effected by a function of the form

$$f(z) = \alpha \int_0^z \frac{dx}{(x - a_i)^{\mu_1} \cdots (x - a_n)^{\mu_n}} + \beta, \tag{1.1}$$

where $a_1 < \cdots < a_n$ are real and $\alpha, \beta \in \mathbb{C}$.

Although there is ample literature on the subject (see, e.g., [1–3], as well as the complete overview contained in Driscoll and Threfethen [4]), a few remarks would not be out of place here. First of all, even though (1.1) gives the appearance of being an explicit formula, there is actually no known relation between the values of the a_i and the lengths of the sides of D. For this reason, when considering an infinite-sided polygon, one needs to justify passage to a corresponding infinite product, which is what we do in what follows.

Also, formula (1.1) is necessary but not sufficient in the sense that for some values of the a_i's, the mapping need not to be one-to-one (see [5]). To establish the necessity, one needs to consider the behavior of $f(z)$ at ∞, a possibility also clearly excluded in the case of infinitely many a_i.

Before proceeding, we review some variations of (1.1). One of the points a_i may be located at ∞, the formula remaining the same, and one of the vertices of the polygon may be at ∞, where we use the relation $\mu_1 + \cdots + \mu_n = 2$. The formula for mapping the unit disc conformally onto D is essentially the same, but with $|a_i| = 1,\ 1 \le i \le n$. The formula for the mapping onto the exterior of the polygon is

$$g(z) = \alpha \int_1^z e^{\lambda x}(x - a_1)^{\mu_1} \cdots (x - a_n)^{\mu_n} \frac{dx}{x^2} + \beta \tag{1.2}$$

with $\lambda = \sum_{i=1}^{n} \mu_i / a_i$.

In this paper, we explore the case in which there are infinitely many points a_i on the real line (or the unit circle) and obtain results for two kinds of "polygons."

1.1. Polygons with an infinite number of sides

This is the case, for example, of an "infinite stairway" with interior angles alternately equal to $\pi/2$ and $3\pi/2$. The formula in this case is

$$f(z) = \int_0^z \sqrt{\tan(x)}dx. \tag{1.3}$$

The zeros of the denominator $\cos(x)$ correspond to $a_i = (2i + 1)\pi/2,\ \mu_i = 1/2$ and those of the numerator $\sin(x)$ to $a_i = i\pi,\ \mu_i = -1/2$.

1.2. Fractals

This is the case, for example, of the interior of the Koch snowflake, for which the formula on the interior of the unit disc turns out to be

$$g(z) = \int_0^z \prod_{n=0}^{+\infty} \left(1 + x^{6\cdot 4^n}\right) dx. \tag{1.4}$$

A similar generalization of (1.2) gives the conformal mapping onto the exterior of the Koch snowflake.

To reproduce the figures in the text, a program such as Derive, Maple, or Mathematica is required; we explain in each case how to obtain these figures.

To our knowledge, formulas of this kind have not previously been considered in the literature, and the initial nature of the present investigation precludes exhaustive results. It is our hope that others will be motivated to seek general theorems along these lines, or at any rate to find explicit mappings of the upper-half-plane onto other infinitely sided polygons.

We mention here the open problem of a half-strip slit along infinite sequences of equal-length line segments emanating from the infinite sides.

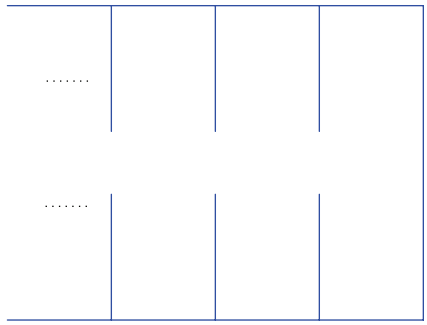

(1.5)

The mapping of the half-plane onto this domain is of importance in the study of differentials on hyperelliptic surfaces of infinite genus as considered in the pioneering work by Myrberg, see [5]. (The formula for the case of the analogously slitted full strip is obtained below.)

2. Polygons with an infinite number of sides

2.1. The infinite staircase

The first example we consider is the mapping defined on the upper half-plane by the formula

$$f(z) = \int_0^z \sqrt{\tan(x)}\, dx. \tag{2.1}$$

The image is given in Figure 1, where the curves shown are the images of horizontal and vertical segments lying in the half-plane; they can be defined directly by

$$\begin{aligned} \alpha(s) = \Bigg(& \mathrm{Re}\left(\mathrm{Numint}\left(\sqrt{\tan(x)},\ x = 0 \text{ to } 0.6 + si\right)\right), \\ & \mathrm{Im}\left(\mathrm{Numint}\left(\sqrt{\tan(x)},\ x = 0 \text{ to } 0.6 + si\right)\right)\Bigg), \quad 0.1 \le s \le 1.1 \end{aligned} \tag{2.2}$$

for a vertical segment, and by

$$\begin{aligned} \beta(s) = \Bigg(& \mathrm{Re}\left(\mathrm{Numint}\left(\sqrt{\tan(x)},\ x = 0 \text{ to } 0.09i + s\right)\right), \\ & \mathrm{Im}\left(\mathrm{Numint}\left(\sqrt{\tan(x)},\ x = 0 \text{ to } 0.09i + s\right)\right)\Bigg), \quad 0.4 \le s \le 10 \end{aligned} \tag{2.3}$$

for a horizontal segment.

The image of the real axis is the infinite staircase with steps of equal length

$$\int_0^{\pi/2} \sqrt{\tan(x)}\, dx = \frac{\pi\sqrt{2}}{2}. \tag{2.4}$$

In order to prove that this formula actually defines a one-to-one mapping, we proceed as follows.

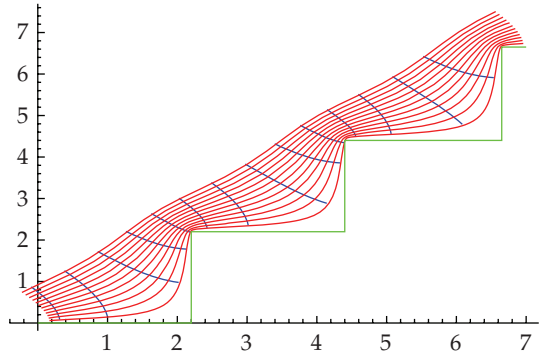

Figure 1: The infinite staircase. $f(z) = \int_0^z \sqrt{\tan\, x}\, dx$.

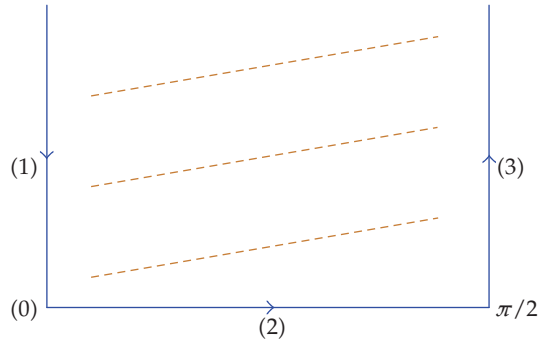

Figure 2

Consider the triangle (i.e., half-strip) of Figure 2.

The image of the positive imaginary axis (labeled (1) in the figure) is given by

$$\int_0^{is} \sqrt{\tan(x)}dx = i \int_0^s \sqrt{\tan(it)}\, dt = \frac{-1+i}{\sqrt{2}} \int_0^s \sqrt{\frac{e^t - e^{-t}}{e^t + e^{-t}}}\, dt \tag{2.5}$$

for $0 \leq s \leq +\infty$, so that it is the half-line making an angle of $3\pi/4$ with the positively oriented real axis. The image of (2) is the real segment $[0, \pi\sqrt{2}/2]$, and that image of (3) is a half-line parallel to the first one and beginning at $\pi\sqrt{2}/2$ as in Figure 3.

Consider the triangle of Figure 3.

The general theory of conformal mappings applies to these two triangles, so that from the bijectivity on the boundaries we can conclude bijectivity in the interior. With the Schwarz reflection principle as applied to the vertical segments (1), (3), and their reflections, the mapping can now be extended to the entire upper half-plane.

The function

$$f(z) = \int_0^z \frac{\sin^\nu(x)}{\cos^\mu(x)}\, dx, \tag{2.6}$$

with $0 < \nu, \mu < 1$, generalizes this to zigzag patterns.

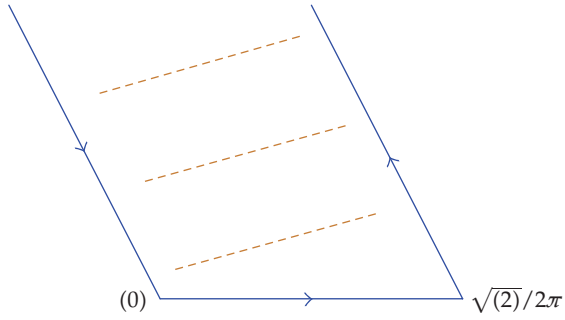

Figure 3

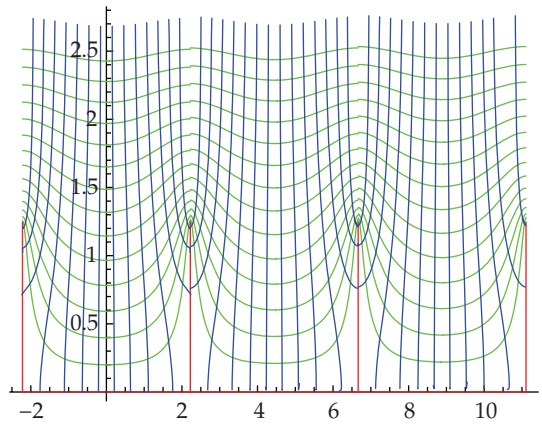

Figure 4: The hairy half-plane, $f(z) = \int_0^z (\cos(x/2)/\sqrt{\cos(x)})\, dx$.

2.2. The hairy half-plane

We next consider interior angles $\pi/2$ at $a_i = (2i+1)\pi/2$ $(i \in \mathbb{Z})$ and 2π at $b_i = (2i+1)\pi$.

The mapping function is therefore

$$f(z) = \int_0^z \frac{\cos(x/2)}{\sqrt{\cos(x)}}\, dx, \tag{2.7}$$

and the image is shown in Figure 4.

To establish that the given mapping is indeed one-to-one, it is first necessary to see that the length of the segment from an angle $\pi/2$ to the tip of the hair is the same on both sides, that is, that

$$\int_{\pi/2}^{\pi} \frac{\cos(x/2)}{\sqrt{-\cos(x)}} dx = \int_{\pi}^{3\pi/2} \frac{-\cos(x/2)}{\sqrt{-\cos(x)}}, \tag{2.8}$$

an equality easily obtained by the change of variable $x \to 2\pi - x$.

The proof can now be completed in the same way as for the infinite staircase by first considering the image of a triangle with vertical sides at π and 3π, and then extending the mapping by the reflection principle.

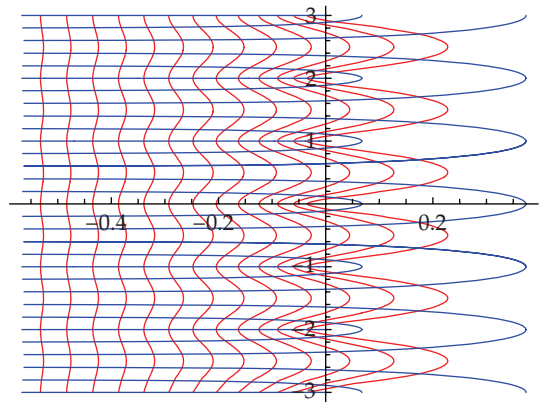

Figure 5: The hairy plane, $f(z) = \int_0^z \tan \pi x \, dx$.

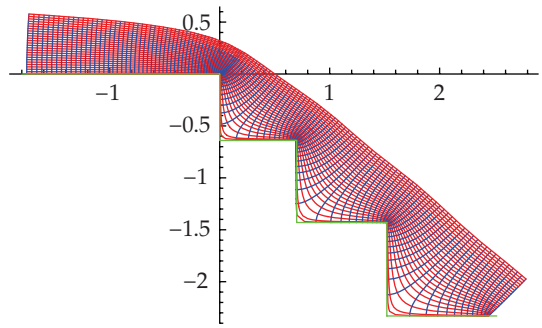

Figure 6: Half a stair or the stairway to the abyss, $f(z) = \int_0^z \sqrt{(\Gamma(1/2 - x)/\Gamma(-x))} \, dx$.

In a similar fashion, we obtain a formula for the hairy plane, which can be regarded as a polygon with infinitely many sides and interior angles alternately equal to 2π and 0.

This means taking

$$f(z) = \int_0^z \frac{\sin(x)}{\cos(x)} \, dx \tag{2.9}$$

as in Figure 5.

2.3. The infinite half-staircase

In order to consider only one half of the stair, we have to take analytic functions in (1.1) having half as many zeros as before, which leads to the Γ function. Indeed, the formula

$$f(z) = \int_0^z \sqrt{\frac{\Gamma(1/2 - x)}{\Gamma(-x)}} \, dx \tag{2.10}$$

defines such a mapping (see Figure 6).

However, to prove that the mapping given in (2.10) is one-to-one, we cannot use the arguments of examples 1 and 2 since there is no symmetry with respect to a line. We proceed as follows. Since

$$\frac{1}{\Gamma(x)} = e^{\gamma x} x \prod_{n=1}^{+\infty} \left(1 + \frac{x}{n}\right) e^{-x/n}, \tag{2.11}$$

it follows that

$$\sqrt{\frac{\Gamma(1/2 - x)}{\Gamma(-x)}} = e^{-\gamma/4} \sqrt{\frac{x}{x - 1/2}} \lim_{N \to +\infty} \prod_{n=1}^{N} \left(\frac{1 - x/n}{1 + (1/2 - x)/n}\right)^{1/2} e^{n/4}. \tag{2.12}$$

The classical Schwarz-Christoffel formula can be applied to each finite product on the right-hand side, which gives a staircase with a finite number of steps. These conformal mappings converge uniformly to the required mapping since for each positive integer, the integral

$$\int_m^{m+1/2} \sqrt{\frac{\Gamma(1/2 - x)}{\Gamma(-x)}}\, dx \tag{2.13}$$

is finite.

To obtain a half-stair with the steps moving to the left one would naturally use

$$\int_0^z \sqrt{\frac{\Gamma(-x)}{\Gamma(1/2 - x)}} dx. \tag{2.14}$$

Finally, to obtain half a hairy plane, we take

$$f(z) = \int_{-1}^{z} \frac{\Gamma(1/2 - x)}{\Gamma(-x)} dx \tag{2.15}$$

as in Figure 7, or half a hairy half-plane via

$$\frac{\sqrt{\Gamma(1/2 - x)}}{\Gamma(-x/2)} \tag{2.16}$$

and so on.

3. Fractals

3.1. The Koch snowflake

Driscoll and Trefethen ([4, Chapter 4.5]) remark that the conformal mapping into the interior or exterior of complicated fractals, such as the Koch snowflake, ought to be treatable in a manner related to the multiple method. In the next theorem, we give an explicit geometric formula which does this.

Numerical schemes have been studied before using iteration procedures, see [6].

The Koch snowflake is obtained as the limit of a sequence of polygons defined as in Steps 1, 2, and 3, and so on.

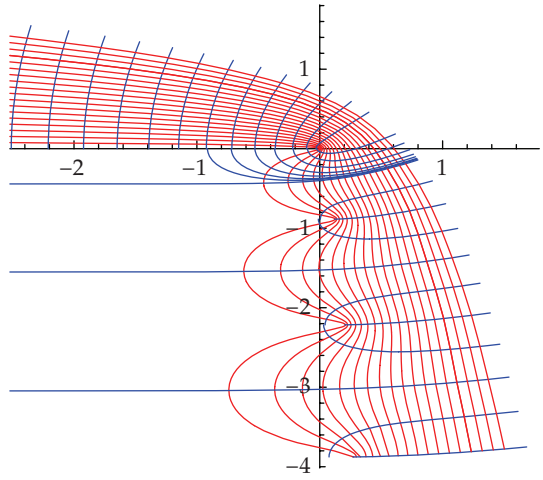

Figure 7: Half a hairy half-plane, $f(z) = \int_{-1}^{z} (\Gamma(1/2 - x)/\Gamma(-x))\, dx$.

Step 1.

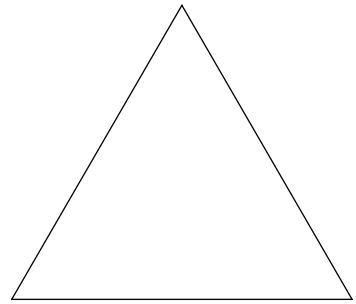

(3.1)

Step 2.

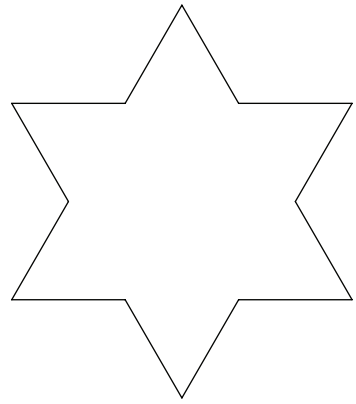

(3.2)

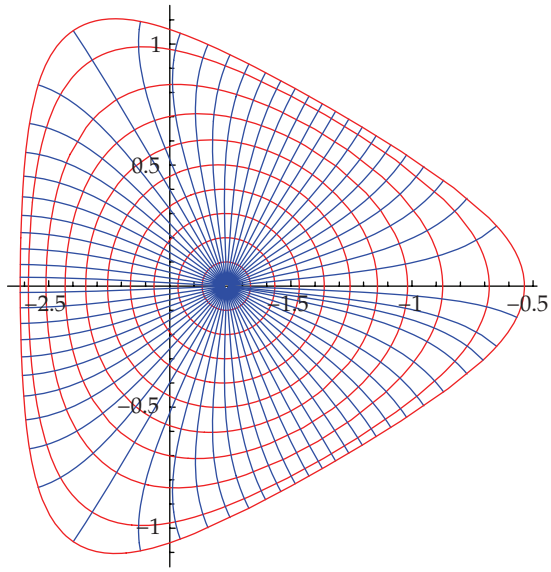

Figure 8: Interior of the Koch snowflake, Step 1.

Step 3.

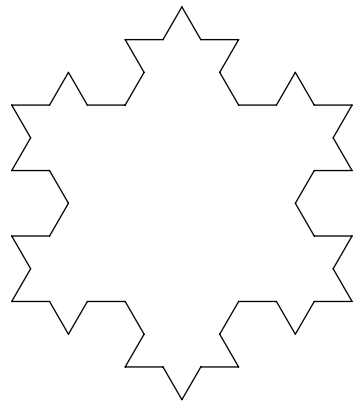

(3.3)

At each step, we consider the Schwarz-Christoffel mapping of the unit disc into the interior of the polygon; we use the notation of the introduction throughout.

Step 1. $\alpha_k = 1/3,\ \mu_k = 2/3,\ a_k = \exp(2\pi ik/3)\ (k = 1,2,3)$;

$$F(z) = \int_1^z \frac{dx}{(x-1)^{2/3}(x-\exp(2\pi i/3))^{2/3}(x-\exp(4\pi i/3))^{2/3}} = \int_1^z \frac{dx}{(x^3-1)^{2/3}}. \tag{3.4}$$

This conformal mapping is portrayed in Figure 8.

Step 2. $a_k = \exp(2\pi ik/12)\ (0 \le k \le 11)$;

$$\begin{aligned} \alpha_k &= \frac{1}{3}, \quad \mu_k = \frac{2}{3}, \quad k = 0,2,4,68,10 \\ \alpha_k &= \frac{4}{3}, \quad \mu_k = \frac{-1}{3}, \quad k = 1,3,57,911. \end{aligned} \tag{3.5}$$

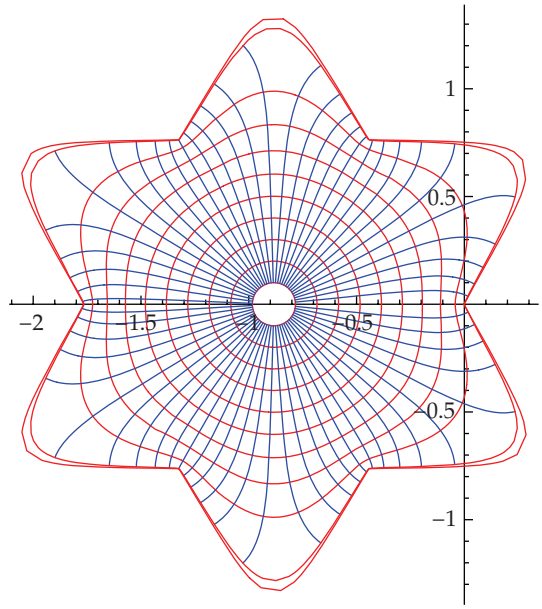

Figure 9: Interior the Koch snowflake, Step 2.

The formula for the conformal mapping is

$$F(z) = \int_1^z \frac{\left(x^6+1\right)^{1/3}}{\left(x^6-1\right)^{2/3}}\,dx \tag{3.6}$$

and the image of the unit disc appears in Figure 9.

Step 3. $a_k = \exp(2\pi ik/48)$ $(0 \le k < 47)$

$$\alpha_k = \frac{1}{3}, \quad \mu_k = \frac{2}{3}, \quad k = 0,2,6,8,10,14,16,18,22,24,26,30,32,34,38,40,42,46,$$
$$\alpha_k = \frac{3}{4}, \quad \mu_k = \frac{-1}{3} \quad \text{all other } k. \tag{3.7}$$

Although the combinatorics is not automatic, the formula for the conformal mapping is

$$F(z) = \int_1^z \frac{\left[\left(x^6+1\right)\left(x^{24}+1\right)\right]^{1/3}}{\left[\left(x^3-1\right)\left(x^3+1\right)\left(x^{12}+1\right)\right]^{2/3}}\,dx, \tag{3.8}$$

the image of the unit disc is given in Figure 10.

We may generalize the following.

Step n. $a_k = \exp(2\pi ik/(3\times 4^n))$, $0 \le k < 3\times 4^n$ with an integrand of the form

$$\frac{\left[\left(x^6+1\right)\left(x^{24}+1\right)\cdots\left(x^{6\cdot 4^{n-1}}+1\right)\right]^{1/3}}{\left[\left(x^3-1\right)\left(x^3+1\right)\left(x^{12}+1\right)\cdots\left(x^{3\cdot 4^{n-1}}+1\right)\right]^{2/3}}. \tag{3.9}$$

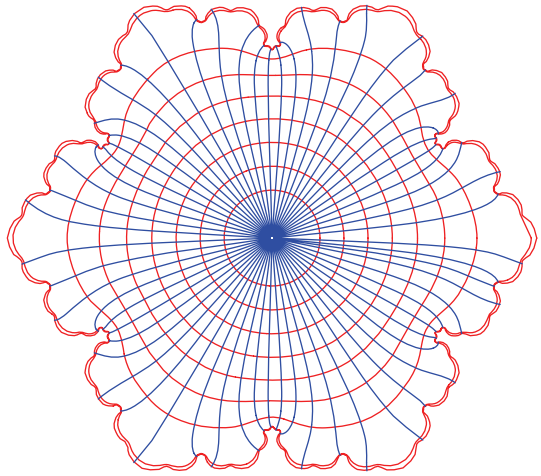

Figure 10: Interior of Koch's snowflake, Step 3.

Theorem 3.1. *The formula for the conformal map from the interior of the unit disc to the interior of a Koch snowflake is*

$$F(z) = \int_0^z \prod_{n=0}^{+\infty} \left(1 + x^{6\cdot 4^n}\right) dx, \quad |z| < 1. \tag{3.10}$$

Proof. The wording "a Koch snowflake" means that it is the limit of polygons with the same angles as the polygons in the Koch pattern, but with unequal sides.

First, we rewrite the integrand for Step n as

$$\left(1 + x^6\right)\left(1 + x^{24}\right) \cdots \frac{\left(1 + x^{6\cdot 4^{n-1}}\right)}{\left(1 - x^{3\cdot 4^n}\right)^{2/3}} \tag{3.11}$$

(modulo a cube root of 1), so that for $|x| < 1$ the integrand converges to the one indicated in the statement of the theorem.

That the lengths are not equal to the lengths in true Koch snowflake can already be seen at Step 3:

Define

$$\begin{aligned} a &= \int_0^1 \frac{\left(1 + x^{24}\right)^{1/3}}{\left(1 - x^{24}\right)^{2/3}} dx = 1.13856, \\ b &= \int_0^1 \frac{x^6 \left(1 + x^{24}\right)^{1/3}}{\left(1 - x^{24}\right)^{2/3}} dx = 0.270237, \end{aligned} \tag{3.12}$$

so that

$$F(1) = a + b \tag{3.13}$$

is one vertex of the polygon. But then

$$F\left(e^{\pi i/6}\right) = e^{\pi i/6}\,(a - b). \tag{3.14}$$

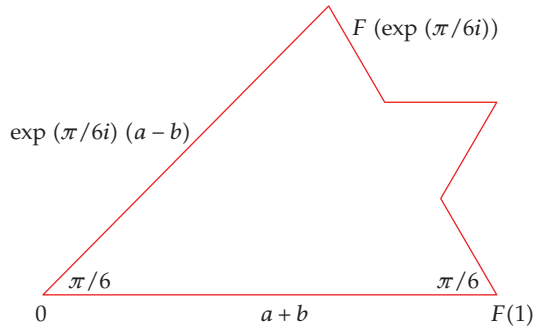

Figure 11

The image of a circular sector from 0 to 1 to $\exp(\pi i/6)$ is therefore a polygon of the form of Figure 11.

If the lengths were equal to those of the regular snowflake then the vertex $F(\exp(\pi i/6))$ would be the vertex of the isosceles triangle with base $a + b$ and base angle $\pi/6$.

The side would equal $(a + b)/\sqrt{3}$. But

$$\frac{(a+b)}{\sqrt{3}} < a - b, \tag{3.15}$$

showing that the second length in the small triangle is necessarily shorter than the first one, leading to a location of $F(\exp(\pi i/6))$ slightly "higher" than it should be.

Observe also that the location of this last vertex implies (the angles being as required) that the map is one-to-one on the boundary and therefore one-to-one throughout.

In general, the image in Step n differs somewhat, but not by too much, from a regular snowflake with all sides equal.

If we analyze a sufficiently general case as in Step 3, say that we have the mapping

$$f(z) = \int_0^z \left(1 + x^6\right)\left(1 + x^{24}\right) \frac{\left(1 + x^{96}\right)^{1/3}}{\left(1 - x^{96}\right)^{2/3}}\, dx. \tag{3.16}$$

It is easy to obtain the points

$$\begin{aligned} P^* &= f(1) = 1.35, \qquad & Q^* &= f\left(e^{\pi i/24}\right), \\ R^* &= f\left(e^{\pi y/8}\right), \qquad & S^* &= f\left(e^{\pi i/6}\right). \end{aligned} \tag{3.17}$$

If we compare them to a regular snowflake with vertices $P,\ Q,\ R,\ S$, we obtain points at a distance smaller than 0.1.

What is to be noticed is that for the image not be one-to-one on the boundary, the point Q^* should differ sufficiently from Q, to be below PO, for example; the position of $P^*,\ Q^*,\ R^*,\ S^*$ thus forces the actual polygon to be free of self-intersections, the angles being $\pi/3$ or $2\pi/3$. We draw one such possible polygon in Figure 12.

The sequence of conformal mappings therefore converges to a nonconstant conformal mapping (since $F'(0) = 1$).

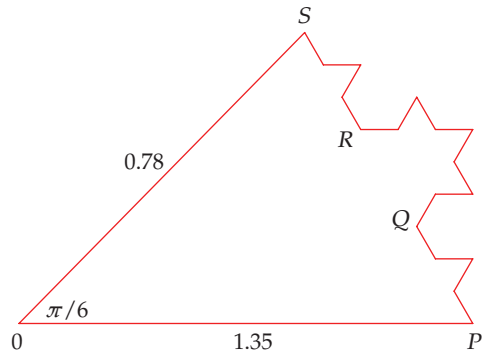

Figure 12

We check that the image is not all of $\mathbb{C}$.
We claim that

$$F(1) = \int_0^1 \prod_{n=0}^{+\infty} (1 + x^{6\cdot 4^n}) dx \leq \frac{3}{4}. \tag{3.18}$$

Indeed, with $y = x^6$, we have $0 \leq y \leq 1$ and

$$\begin{aligned} (1+y)(1+y^4)(1+y^{16})\cdots &= 1 + y + (y^4 + y^5) + (y^{16} + y^{17} + y^{20} + y^{21}) + \cdots \\ &\leq 1 + y + 2y^4 + 4y^{16} + \cdots \\ &= 1 + \sum_{n=0}^{\infty} 2^n y^{4^n}. \end{aligned} \tag{3.19}$$

Thus the integral is bounded from above by

$$\int_0^1 1 + \sum_{n=0}^{+\infty} 2^n x^{4^n \cdot 6}\, dx = 1 + \sum_{n=0}^{+\infty} \frac{2^n}{6\cdot 4^n} \leq 1 + \frac{1}{6} \sum_{n=0}^{+\infty} \frac{1}{2^n} = \frac{4}{3}. \tag{3.20}$$

We also check that the image is not a disc.
Set

$$a = \int_0^1 \prod_{n=1}^{+\infty} (1 + x^{6\cdot 4^n})\, dx, \qquad b = \int_0^1 x^6 \prod_{n=1}^{+\infty} (1 + x^{6\cdot 4^n})\, dx. \tag{3.21}$$

Then $F(1) = a + b$ and $0 < b < a$.
But

$$F\left(e^{\pi i/6}\right) = e^{\pi i/6}(a - b) \tag{3.22}$$

has modulus smaller than $F(1)$.

Finally, we have to explain a subtle point that arises in producing a drawing such as the one in Figure 10.

One cannot write, for example,

$$\left(1+x^6\right)^{1/3}\left(1+x^{24}\right)^{1/3} = \left[\left(1+x^6\right)\left(1+x^{24}\right)\right]^{1/3} \tag{3.23}$$

since the branch we implicitly use by analytic continuation may not coincide with the fixed branches of the mathematical software.

With

$$\begin{aligned} u(k,x) &= \log\left(\exp\left(\frac{\pi i k}{24}\right) - x\right), \\ v(k,x) &= \log\left(x - \exp\left(\frac{\pi i k}{24}\right)\right), \end{aligned} \tag{3.24}$$

the numerator of the integrand is

$$\begin{aligned} \mathrm{Num}(x) = \exp\big(1/3(&u(1,x)+u(3,x)+u(3,x)+u(4,x)+u(5,x) \\ &+u(7,x)+u(9,x)+u(11,x)+v(12,x)+v(13,x) \\ &+v(15,x)+v(17,x)+v(19,x)+v(20,x) \\ &+v(21,x)+v(23,x)+v(25,x)+v(27,x) \\ &+v(28,x)+v(29,x)+v(31,x)+v(33,x)+v(35,x) \\ &+v(36,x)+u(37,x)+u(39,x)+u(41,x)+u(43,x) \\ &+u(44,x)+u(45,x)+u(47,x))\big); \end{aligned} \tag{3.25}$$

and the denominator is

$$\begin{aligned} \mathrm{Den}(x) = \exp\big(2/3(&u(0,x)+u(2,x)+u(6,x) \\ &+u(8,x)+u(10,x)+v(14x)+v(16,x) \\ &+v(18,x)+v(22,x)+v(24,x)+v(26,x) \\ &+v(30,x)+v(32,x)+v(34,x)+u(38,x) \\ &+u(40,x)+u(42,x)+u(46,x))\big). \end{aligned} \tag{3.26}$$

At any rate, the formula of the theorem with terms of up to $6\cdot 4^6$ is sufficiently precise (and simpler to use) and gives Figure 13. □

3.2. The exterior of the snowflake

At Step 1, we use the formula of the introduction with $a_k = \exp(2\pi i/3 \times k)$, $\mu_k = 2/3$, $1 \le k \le 3$.

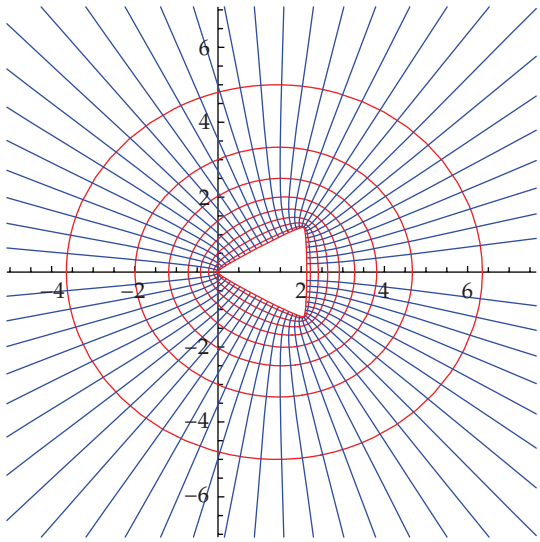

Figure 13: Exterior of the Koch snowflake, Step 1.

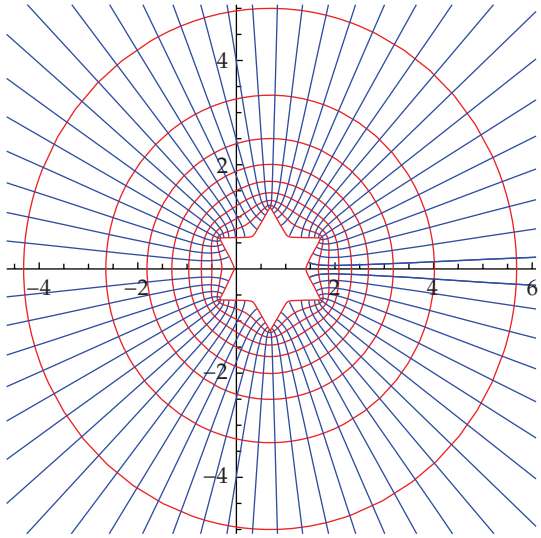

Figure 14: Exterior of the Koch snowflake, Step 2.

In this case, $\lambda = 2/3 \sum_{k=1}^{3} d_k = 0$ so that the formula is

$$F(z) = \int_1^z (x^3 - 1)^{2/3(dx/x^2)} \tag{3.27}$$

whose image is in Figure 14.

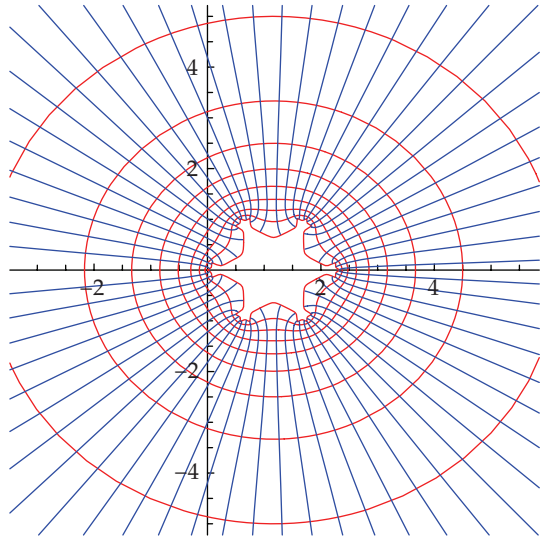

Figure 15: Exterior of the Koch snowflake, Step 3.

In the same way, the formulas for Steps 2 and 3 are

$$\int_1^z \frac{\left[\left(x^3-1\right)\left(x^3+1\right)\right]^{2/3}}{\left[\left(x^6+1\right)\right]^{1/3}}\frac{dx}{x^2},$$
$$\int_1^z \frac{\left[\left(x^3-1\right)\left(x^3+1\right)\left(x^{12}+1\right)\right]^{2/3}}{\left[\left(x^6+1\right)\left(x^{24}+1\right)\right]^{1/3}}\frac{dx}{x^2}, \tag{3.28}$$

corresponding to Figures 15 and 16.

The mapping from the unit disc to the exterior of the Koch snowflake is given by

$$F(z)=\int_1^z \left(\prod_{n=0}^{+\infty}\left(1+x^{6\cdot 4^n}\right)\right)^{-1}\frac{dx}{x^2}. \tag{3.29}$$

3.3. Periodic Koch fractals

In a paper on diffusive transport by Brady and Pozrikidis (cf. [6]) the authors consider conformal mappings of a rectangle onto regions $R_m,\ m=1,2,\ldots$ as in Figure 16.

The mappings can then be extended by reflections on the vertical sides to mappings from an infinite strip to regions bounded below by the given contours. In the limit, a fractal region is obtained.

The mapping is given by an iteration procedure which we summarize as follows.

$$\text{Define } G(\xi)=\prod_{n=0}^{N}\left(\prod_{k=-\infty}^{+\infty}\sin h\left(\frac{\pi}{2h}\left(\xi-a_n-ka_N\right)\right)\right)^{\alpha_n}. \tag{3.30}$$

(i) Guess initial values $a_i,\ i=1,\ldots,N$.

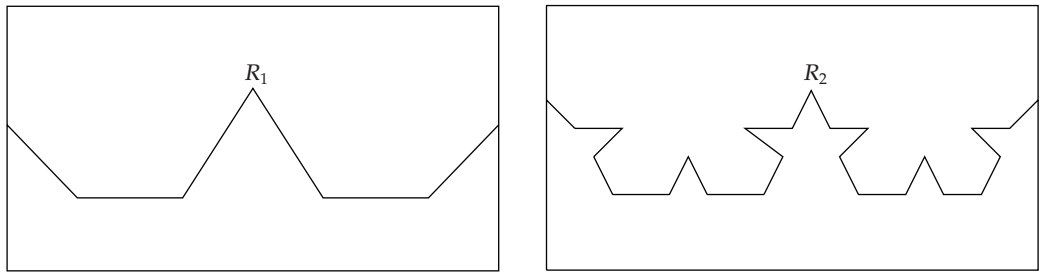

Figure 16

(ii) Locate the vertices on the triangular contours by

$$Z_n^G = Z_{n-1}^G + R\int_{a_{n-1}}^{a_n} G(\xi)d\xi \tag{3.31}$$

and compare them to the known exact values of the vertices a_n. If they are equal the calculation stops; otherwise compute improved values for a_n using the corrector formula:

$$\left|a_n^{\text{new}} a_{n-1}^{\text{new}}\right| = \left|a_n^{\text{old}} - a_{n-1}^{\text{old}}\right| \left|\frac{Z_n - Z_{n-1}}{Z_n^G - Z_{n-1}^G}\right|. \tag{3.32}$$

This procedure works well in the first few iterations but, as the authors explain, is computationally prohibitive already for $m = 5$ (cf. [6] for details).

Using the Schwarz-Christoffel formula in a similar way as in number 2 above, we may define a conformal mapping to a region bounded below by a periodic fractal of Koch's type obtained from Figure 16. For $m = 1$ consider the function

$$F(z) = \int_0^z \frac{\left(1 - e^{2\pi i x/3}\right)}{\left(1 - e^{2\pi i}\right)^{1/3}} dx. \tag{3.33}$$

It maps the upper half plane to a region bounded by the periodic contour as in R_1 (extended by reflection on the vertical sides).

The actual lengths of the sides in the image are $\{1, 2, 1\}$ so that they do not coincide with preassigned value 1 for all sides, but the image has the same geometrical shape.

For $m = 2$, the function is defined by

$$\int_0^z \frac{\left(1 - e^{2\pi i x/3}\right)}{\left(1 - e^{2\pi i x}\right)^{1/3}} \frac{\left(1 + e^{2\pi i x}\right)^{2/3}}{\left(1 + e^{4\pi i x}\right)^{1/3}} dx \tag{3.34}$$

and in the limit, for $\operatorname{Im} z > 0$,

$$\int_0^z \frac{\left(1 - e^{2\pi i x/3}\right)}{\left(1 - e^{2\pi i x}\right)^{1/3}} \frac{\prod_{n=0}^{+\infty}\left(1 + e^{2\pi i 4^n x}\right)^{2/3}}{\prod_{n=0}^{+\infty}\left(1 + e^{4\pi i 4^n x}\right)^{1/3}} dx. \tag{3.35}$$

The infinite products converge uniformly in compact sets on the upper half plane and the integral defines a conformal map onto a region bounded below by an infinite periodic fractal of Koch type. As usual with these maps, we cannot so far control precisely the lengths of the sides except numerically for the first few steps.

3.4. A tree

We define a sequence of "trees" as follows.

Step 1.

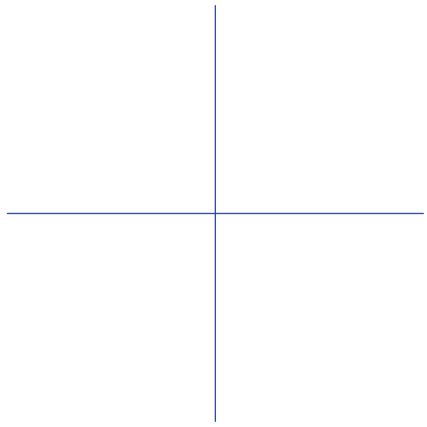

(3.36)

Step 2.

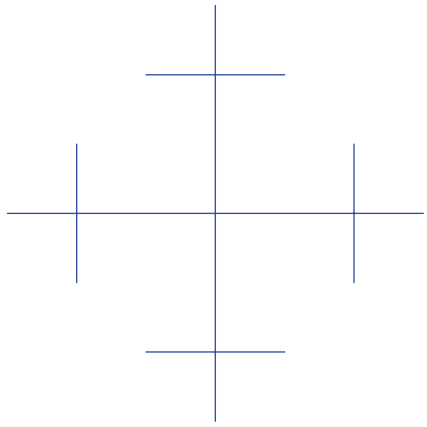

(3.37)

Step 3.

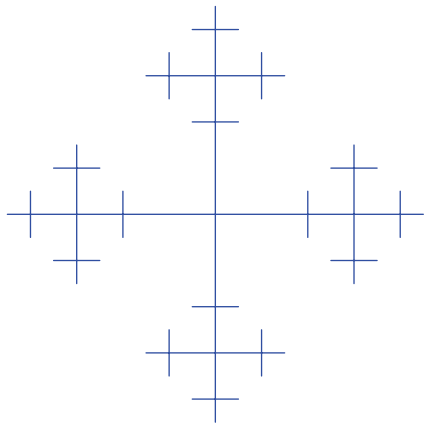

(3.38)

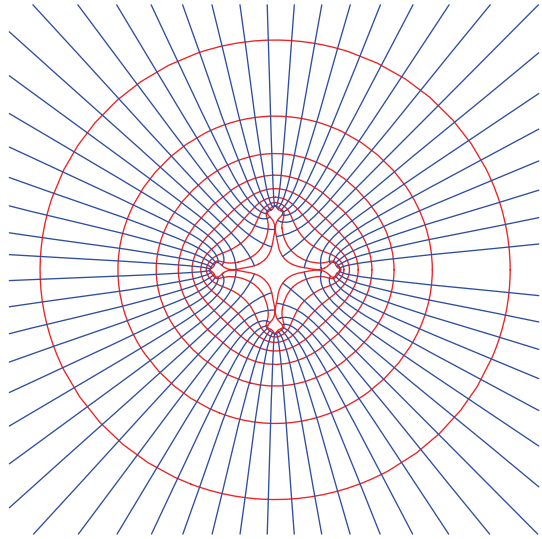

Figure 17: Exterior of a tree, Step 3.

We want to define a sequence of Schwarz-Christoffel mappings from the unit disc to the complements of these trees.

The interior angles at Step 1 give $\alpha_1 = \alpha_3 = \alpha_5 = \alpha_7 = 0$ with $\mu_1 = \mu_3 = \mu_5 = \mu_7 = 1$ at the points and $\alpha_2 = \alpha_4 = \alpha_6 = \alpha_8 = 3/2$, $\mu_2 = \mu_4 = \mu_6 = \mu_8 = -1/2$ at the corners.

Therefore

$$F(z) = \int_1^z \frac{1+x^4}{\left(1-x^4\right)^{1/2}} \frac{dx}{x^2} \tag{3.39}$$

is the required formula at Step 1.

At Step 2, we obtain

$$F(z) = \int_1^z \frac{1+x^4}{\left(1-x^4\right)^{1/2}} \frac{1+x^8}{\left(1+x^{16}\right)^{1/2}} \frac{dx}{x^2} \tag{3.40}$$

with branches at the 32 roots of unity.

Similarly, at Step 3

$$F(z) = \int_1^z \frac{1+x^4}{\left(1-x^4\right)^{1/2}} \frac{\left(1+x^8\right)\left(1+x^{32}\right)}{\left[\left(1+x^{16}\right)\left(1+x^{64}\right)\right]^{1/2}} \frac{dx}{x^2}. \tag{3.41}$$

The image is shown in Figure 17.

In the limit, we obtain the formula

$$F(z) = \int_1^z \frac{1+x^4}{\left(1-x^4\right)^{1/2}} \frac{\prod_{n=1}^{+\infty}\left(1+x^{2\cdot 4^n}\right)}{\left[\prod_{n=1}^{+\infty}\left(1+x^{4^{n+1}}\right)\right]^{1/2}} \frac{dx}{x^2} \tag{3.42}$$

for the conformal mapping of the unit disc onto the exterior of this fractal.

There are of course many more trees to be considered but the combinatorics arising from angles and points is not straightforward, so that it may be hard to obtain a general expression for the conformal mapping. We leave these as questions for further study.

4. Conclusion

The classical Schwarz-Christoffel formula maps the upper half plane to a polygon with prescribed angles, but with sides of unknown lengths. Notwithstanding this, we have shown that the formula can be extended to a variety of shapes with an infinite number of vertices, namely, stairs, slitted planes, fractals of Koch's type and trees. It would be very interesting in the future to find exactly the branch points necessary in Koch snowflake as well as in specific slitted regions.

Acknowledgment

This research was partially suported by Fondecyt 1050904.

References

[1] D. Bonciani and F. Vlacci, "Some remarks on Schwarz-Christoffel transformations from the unit disk to a regular polygon and their numerical computation," *Complex Variables and Elliptic Equations*, vol. 49, no. 4, pp. 271–284, 2004.

[2] P. Henrici, *Applied and Computational Complex Analysis. Vol. 1: Power Series, Integration, Conformal Mapping, Location of Zeros*, Pure and Applied Mathematics, John Wiley & Sons, New York, NY, USA, 1974.

[3] E. Johnston, "A "counter example" for the Schwarz-Christoffel transform," *The American Mathematical Monthly*, vol. 90, no. 10, pp. 701–703, 1983.

[4] T. A. Driscoll and L. N. Trefethen, *Schwarz-Christoffel Mapping*, vol. 8 of *Cambridge Monographs on Applied and Computational Mathematics*, Cambridge University Press, Cambridge, UK, 2002.

[5] P. J. Myrberg, ""Uber analytische Funktionen auf transzendenten zweibl"attrigen Riemannschen Fl"achen mit reellen Verzweigungspunkten," *Acta Mathematica*, vol. 76, no. 3-4, pp. 185–224, 1945.

[6] M. Brady and C. Pozrikidis, "Diffusive transport across irregular and fractal walls," *Proceedings of the Royal Society of London. Series A*, vol. 442, no. 1916, pp. 571–583, 1993.